Simulation of Atom Focusing for Nanostructure Fabrication

Chang Jae Lee

Department of Chemistry, Sunmoon University, Asan 336-840, Korea
Received January 24, 2003

The light pressure force from an optical standing wave (SW) can focus an atomic beam to submicrometer dimensions. To make the best of this technique it is necessary to find a set of optimal experimental parameters. In this paper we consider theoretically the chromium atoms focusing and demonstrate that the focusing performance depends not only on the strength of but also on the time atoms take to traverse the force field. The general conclusions drawn can easily be applied to other atoms. To analyze the problem we numerically integrate a coupled time-dependent Schrödinger equation over a wide range of experimental parameters. It is found that an optimal atomic beam speed-laser intensity pair does exist, which could give substantially improved focusing over the one with the experimental parameters given in the literature. It is also shown that the widely used classical particle optics approach can lead to erroneous predictions.

Key Words : Atom lithography, Nanofabrication, Atom manipulation, Atom-laser interaction

Introduction

The development of fabrication techniques of artificially generated nanostructures holds a great promise for the next-generation technology. At present, there exits a variety of techniques for nanostructure fabrication. These techniques include molecular-beam epitaxy and electron-beam and optical lithography. These conventional lithography techniques remove atoms from a substrate, thus being "invasive" techniques. In the last decade the focusing of neutral atoms by use of near-resonant light fields has been the subject of intense research activities. This has been driven to a large extent by the possibility of generating focal spots on the nanometer scale by use of specially configured laser intensity profiles. The high-resolution focusing of atomic beams followed by noninvasive deposition of these atoms onto a substrate has emerged as a promising nanofabrication technique,[1,2] and this technique has been termed "atom lithography".[3] Seideman has developed a similar technique for lithography with molecules.[4] As a consequence of the small de Broglie wavelength, atom lithography has the potential to achieve extremely high resolution.[5]

The analysis of atom lithography has usually been based on classical particle optics (CPO).[2,6-8] However, they can not adequately handle more subtle nonclassical effects, and recently quantum mechanical treatments began to appear in the literature.[9,10] It has been shown that for the case of chromium atom some 40% of the width of the deposition profile comes from the wave nature of the atom, and that further refinements in choosing experimental parameters are necessary to minimize the spot size of the deposited atoms.[10] The deposition profile depends on several parameters that may be controlled experimentally. They include the laser power, the detuning between the applied laser and the atomic transition frequencies, substrate position in the SW along the atomic beam direction, and the atomic source beam speed. The first two determine, among other things, the shape and the depth of the force field, and the last two determine the length of time the field exerts on atoms.

The purpose of this paper is to provide guidelines for the optimal atom focusing with the aid of quantum mechanical simulation of the atomic dynamics in a laser SW. The simulation method is described in Section II. The CPO approach is also briefly described in that section. In Section III we consider the deposition of chromium atoms, which has been studied extensively based on the CPO approach.[2,6-8] We give a direct comparison between the quantum-mechanical simulations and the ones with the CPO for the experimental parameters given in the literature. Then we show how the atomic dynamics varies as both the laser power and the atomic beam speed are changed. Again, the results of quantum mechanical and CPO simulations are compared. Finally, in Section IV a summary of our work is given.

Theory of Atom Focusing

The force on an atom exerted by light has been studied extensively in the literature.[11] In general, the force felt by an atom in a light field has both velocity-dependent and conservative terms. The velocity-dependent terms, which arise from Doppler shifts experienced by the atom and from nonadiabatic effects, have been utilized for laser cooling.[12] Many practical applications, such as the slowing and trapping of atoms and the collimation of atomic beams to a high degree, have made use of these dissipative terms. On the other hand, for a wide range of parameters the velocity-dependent terms in the light force can be ignored. In this regime the remaining light force is often referred to as the dipole force,[13] and this is the force that can be utilized to focus atoms. The dipole force derives from a conservative (optical) potential. We review below how we approach the atom focusing, following Ref. [10].

Assume that the atoms move along Oz (the longitudinal

direction) and the single mode SW is applied along Ox (the transverse direction). The y dimension is not considered in this work. The SW may be written in the form

$$\mathbf{E}(x, z; \tau) = 2\boldsymbol{\varepsilon}\mathcal{E}(z)\cos kx \cos \omega\tau . \quad (1)$$

where k, w, $\boldsymbol{\varepsilon}$, and $\mathcal{E}(z)$ are, respectively, the wavevector, the frequency, the polarization, and the amplitude profile of the laser along Oz. The SW has a fast variation along Ox with a periodicity given by the optical wavelength $\lambda = 2\pi/k$, while it has a slower variation along Oz given, as usual, by a Gaussian function[8]

$$\mathcal{E}(z) = \mathcal{E}_0 \exp(-z^2/w_0^2) . \quad (2)$$

In the above $\mathcal{E}_0$ is the peak amplitude and w_0 is the $1/e^2$ radius at the beam waist.

If the longitudinal velocity of the atom v_z is large enough, the motion of the atom along Oz may be treated classically. Furthermore, the light force along Oz is negligible as compared with that along Ox. Thus, v_z is virtually undamped by the interaction with the SW and hence the transit time may be written as $t_u = L/v_z$, where L is the characteristic length of interaction of the atom with the laser. The laser intensity drops to 1% of the peak value at $\pm 1.5\, w_0$ about the Gaussian beam center, so we will take $L = 3\, w_0$. From these discussions it follows that $\mathcal{E}(z)$ may be replaced by the temporal profile

$$\mathcal{E}(t) = \mathcal{E}_0 \exp\left[-\frac{(v_z t - 3w_0/2)^2}{w_0^2}\right] . \quad (3)$$

Now consider a beam of atoms, each having a closed two-level structure

$$\Psi(x, t) = \begin{bmatrix} \psi_e(x, t) \\ \psi_g(x, t) \end{bmatrix} . \quad (4)$$

In the above equation $\psi_g(x, t)$ and $\psi_e(x, t)$ denote the wavefunctions of the center of mass corresponding to the lower state $|g\rangle$ and the upper state $|e\rangle$ of the atom along Ox. For optical transitions the relative upper state population of the atoms in a beam is negligible. Thus we assume that the atoms are initially in $|g\rangle$ with the center-of-mass wavefunction given by a plane wave to simulate a spatially uniform beam $\psi_g(x, 0) \sim \exp(ik_0 x)$, where $\hbar k_0$ is the initial transverse momentum of the atom. We consider only the perfectly collimated beam with no transverse momentum, so we take $k_0 = 0$.

For the experimental parameters considered in this paper spontaneous emission is not so significant as to alter the location of the focal plane.[10] Thus, we may treat the atomic evolution using the regular time-dependent Schrödinger equation. In the SW field atoms experience the dipole force that is proportional to the amplitude gradient of the field.[13] The equation that governs the dynamics of a two-level atom is given by

$$i\hbar\frac{\partial}{\partial t}\Psi(x, t) = \left[\frac{p_x^2}{2m} - \hbar\Delta S_z + \hbar\Omega(x, t)S_x\right]\Psi(x, t) . \quad (5)$$

where p_x is the atomic momentum in the transverse direction, m is the atomic mass. $\Delta = \omega - \omega_A$ is the detuning between the laser frequency and the atomic transition frequency ω_A, and $S_\alpha (\alpha = x, y, z)$ are spin-1/2 operators for the atomic internal states. The atom-laser coupling has been expressed in terms of the local Rabi frequency defined by $\Omega(x, t) = -[2\mathbf{d}\cdot\boldsymbol{\varepsilon}\mathcal{E}(t)\cos kx]/\hbar$, where $\mathbf{d}$ is the dipole moment of the atom relevant to the transition $|g\rangle \leftrightarrow |e\rangle$.

In the CPO approach the atom is assumed to remain adiabatically in the lower state (the validity of the adiabaticity is demonstrated in Ref. [10] and is under the influence of the optical potential. The potential takes the form when the atom-laser system reaches a steady state [11,13,14]

$$U(x,t) = \frac{\hbar\Delta}{2}\ln\left(1 + \frac{2\Omega^2}{4\Delta^2 + \gamma^2}\right) \quad (6)$$

where γ is the decay rate of the atom. Equation (6) should be good for times sufficiently longer than the radiative lifetime $\tau_R = 1/\gamma$ but much shorter than the damping time of the atomic velocity, which is on the order of the recoil time $t_{rec} \equiv 2m/(\hbar k^2)$. (See the discussion in Ref. [13].). The CPO approach uses the ray-tracing equation to describe the atomic dynamics

$$\frac{d^2x}{dt^2} = -\frac{1}{m}\frac{\partial U}{\partial x} \quad (7)$$

where $x(t)$ is the individual trajectory of the atom. Figure 1 shows a shape of the optical potential given above. Atoms are attracted to the bottom of the potential, as we will show in the following section using both the CPO and quantum mechanics.

Analysis of Cr Atom Focusing

A. Experimental Parameters and Atomic Dynamics

Experimental Parameters. The relevant transition for the chromium atom focusing is ${}^7S_3 \rightarrow {}^7P_4^0$, and the corresponding

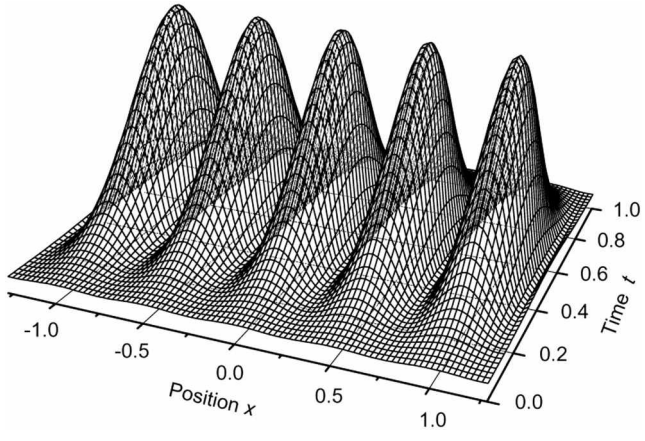

Figure 1. Shape of the optical potential (not to scale). It has a slowly-varying Gaussian profile along the longitudinal direction (the "Time" axis), while it has a much faster variation along the transverse direction (the "Position" axis). Atoms are attracted to the bottom regions of the potential.

wavelength is 425.55 nm. Other parameters taken from Ref. [8] are: decay rate = 5.0 (in 2 π MHz), saturation intensity = 8.5 mW/cm^2, detuning = 200 (in 2 π MHz), SW intensity = 1.98×10^5 W/m^2, polarization = circular (σ^+), $1/e^2$ radius of SW = 0.195 mm, oven temperature = 1800 K.

For convenience of calculations we express the lengths in units of λ, and time and frequencies in recoil units t_{rec} and $\omega_{rec} \equiv 1/t_{rec}$, respectively. For Cr atoms $t_{rec} = 7.51 \times 10^{-6}$ sec and $\omega_{rec} = 2\pi \times 21.2$ kHz. The most probable speed of the atoms emerging from an oven at 1800 K is 926 m/sec, which we regard as the speed of the monoenergetic atomic beam. For the $1/e^2$ radius of 0.195 mm the interaction length L = 0.585 mm, so the corresponding transit time $t_{tr} = 6.32 \times 10^{-7}$ sec = 0.084 t_{rec}. The radiative lifetime $\tau_R = 4 \times 10^{-3}\ t_{rec}$, so $\tau_R << t_{tr} << t_{rec}$ – a regime in which the optical potential of the form Eq. (6) may be applicable. Given γ, the saturation intensity I_s, and the peak SW intensity I_0, the peak Rabi frequency can be calculated to yield $\Omega_0 = 2\pi \times 170.6$ MHz. In recoil units $\gamma = 236\ \omega_{rec}$, $\Delta = 9434\ \omega_{rec}$, and $\Omega_0 = 8047\ \omega_{rec}$.

Particle Optics Simulation. The result of CPO simulation with the above parameters is shown in Figure 2. For the figure we computed numerically 2000 classical trajectories, initially uniformly distributed over $0 \le x \le 0.5\lambda$. The grid size along Ox is 2.5×10^{-4} in units of λ, so digital resolution is about 0.1 nm. We find from the figure that the focal plane is located at the center of the Gaussian profile of the potential, where the atomic density profile is almost like a δ-function. Actually, the feature width is less than the digital resolution, the only deviation from perfect focusing being some pedestal at the base of the peak that is due to anharmonicity of the potential. The experimental parameters

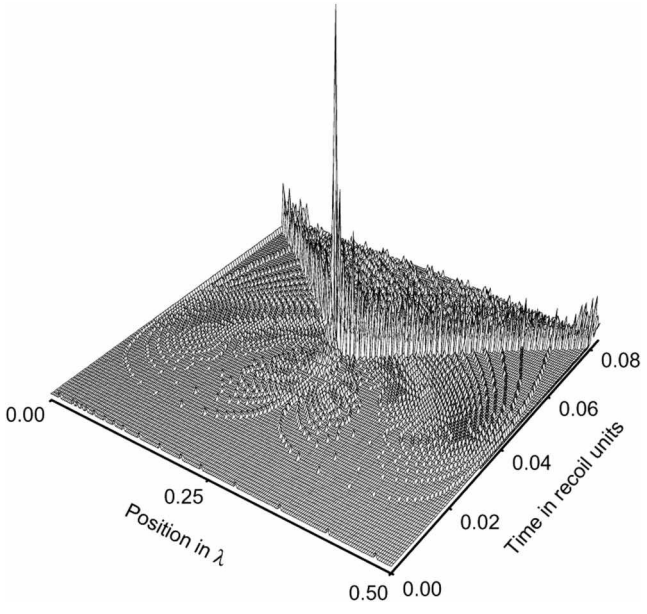

Figure 2. Evolution of the atomic density as predicted by the classical particle optics. Rays converge at the center of the Gaussian profile of the potential, which can be thought to be the focal plane of the thick immersive lens, and beyond that the rays diverge. The experimental parameters given in Sec. IIIA are used.

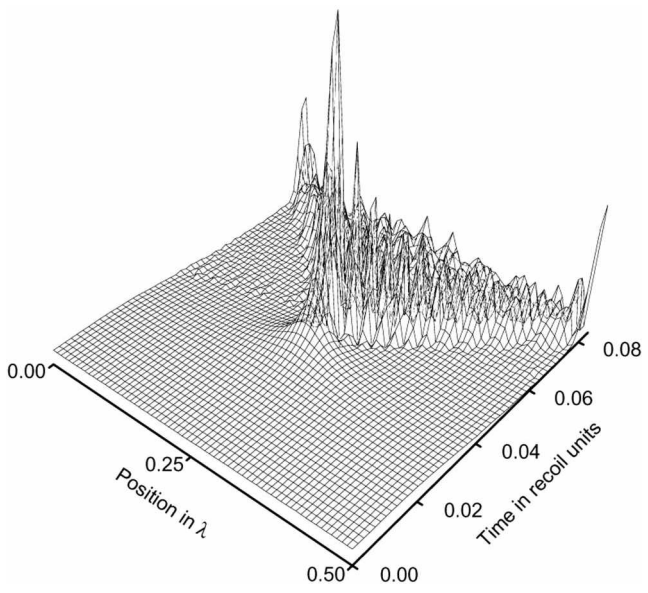

Figure 3. Same as with Fig. 2 but calculated with quantum mechanics. Atoms are first focused to a narrow spot and after that they show an interference pattern, which are absent in the case of particle optics.

are optimal as long as CPO simulation is concerned: when either the detuning or the Rabi frequency is changed, focusing quality degrades.

Wave Mechanical Simulation. Equation (5) is a coupled partial differential equation that can be solved by various techniques, and we choose the algorithm given in Ref. [15]. The output is the square of the wave function $|\Psi(x, t)|^2$,[16] and is shown in Figure 3. For direct comparison with the CPO simulation, all the parameters are kept the same. Due to the wave nature of atom the atomic dynamics deviates strongly from the classical result and the density profile at the center of the Gaussian potential exhibits a diffractive aberration about 8 nm. In addition, the focal plane is not at the center of the Gaussian potential but shifted somewhat downstream. The focal plane may be brought back to the Gaussian center by increasing the laser power, which also results in an increase of resolution and contrast of the density profile.[10] Consequently, optimized parameters based on CPO may not be truly optimal.

B. Effects of Laser Power and Atomic Beam Speed

As we mentioned at the Introduction atom focusing depends on both the optical potential and the length of time the atom takes to traverse the potential. In this section we consider the effects of both the laser power and the atomic beam speed, keeping all other parameters the same. In experiments the beam speed may be easily controlled by changing the temperature of the oven, from which atoms emerge. The beam speeds considered here range from 1/8 to 8 times the original speed and we numerically optimize the laser power (even for the case having the original speed) so as to give the best focusing profile for each beam speed.

The results of quantum mechanical simulations are shown in Figure 4. The curves marked "A" to "G" correspond to the beam speed 1/8 to 8 times the original speed, with the speeds

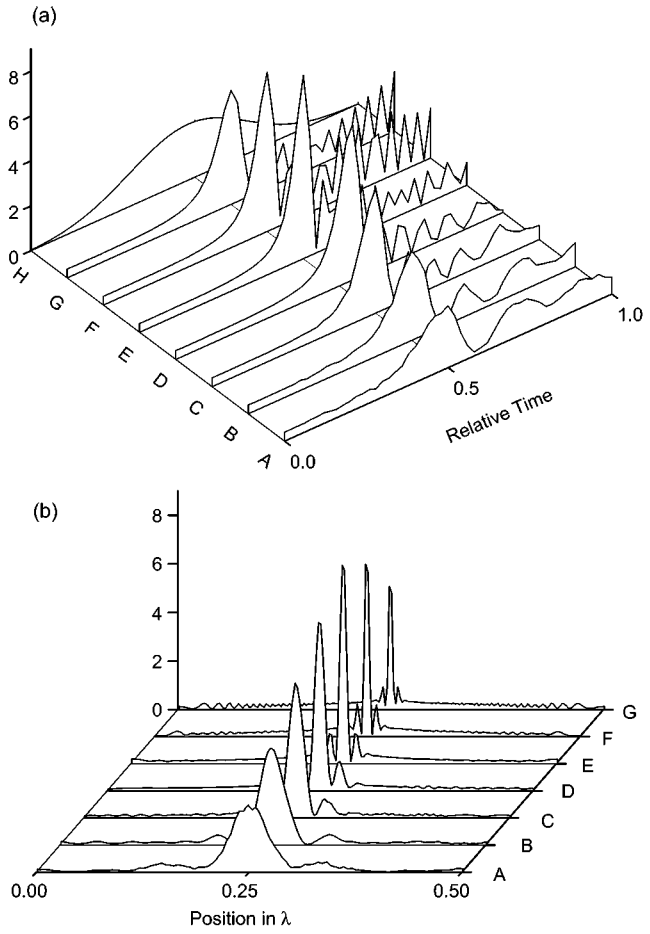

Figure 4. Comparison of the atomic density profile $|\psi(x, t)|^2$ for various atomic beam speeds with optimized laser power: (a) at $x = \lambda/4$, (b) at $t = t_f$, the focal plane. All other parameters are the same as in the previous figures. Curves "A" to "G" correspond to beam speeds 1/8 to 8 times the original speed. Curve "H" is the Gaussian profile of the potential. Note that in (a) the relative time is given by t/t_{tr}, and the focal planes are located at the Gaussian center of the potential.

between the neighboring curves differing by a factor of 2. In Figure 4(a) the curve "H" denotes the Gaussian profile of the optical potential (not to scale) and the rest of the curves show the atomic densities at $x = 0.25\lambda$ as a function of the relative time t/t_{tr}. Figure 4(b) shows the atomic densities about $x = 0.25\lambda$ at $t = t_f$, the time corresponding to the focal plane for each beam speed. We find from the figure that with optimal laser powers the focal planes coincide with the Gaussian center of the potential. In general, the use of slower beams does not lead to improved focusing at all. Faster beams tend to perform better, especially the beam that has twice the current experimental speed (curve "E") is shown to give a superior focusing performance. To be more quantitative we performed a detailed peak analysis for these laser power-atomic beam speed pairs, and the result is shown in Figure 5. It shows that as the beam speed gets slower the width gets broader and, overall, the best focusing is achieved when the beam speed is doubled. The optimized peak Rabi frequency for this double-speed beam is $18000 \times \omega_{rec}$. Note the poor focusing with the current experimental parameters that are

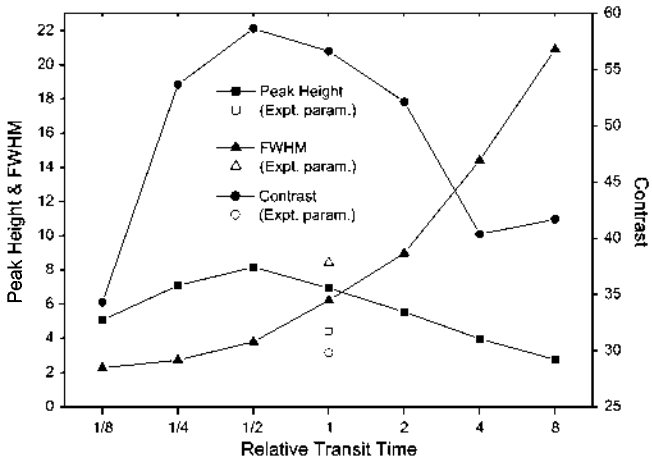

Figure 5. Detailed analysis of the atomic density profiles for various beam speeds. The beam speed is expressed in terms of the relative transit time, $t_{tr}/0.084t_{rec}$. Peaks with bigger heights and contrasts, and narrower widths (FWHM) are better. Note that the best focusing performance is obtained when the speed is doubled and that the parameters in Sec. IIIA (labeled Expt. param. in the figure) give very poor focusing because of the unoptimized laser power-beam speed pair.

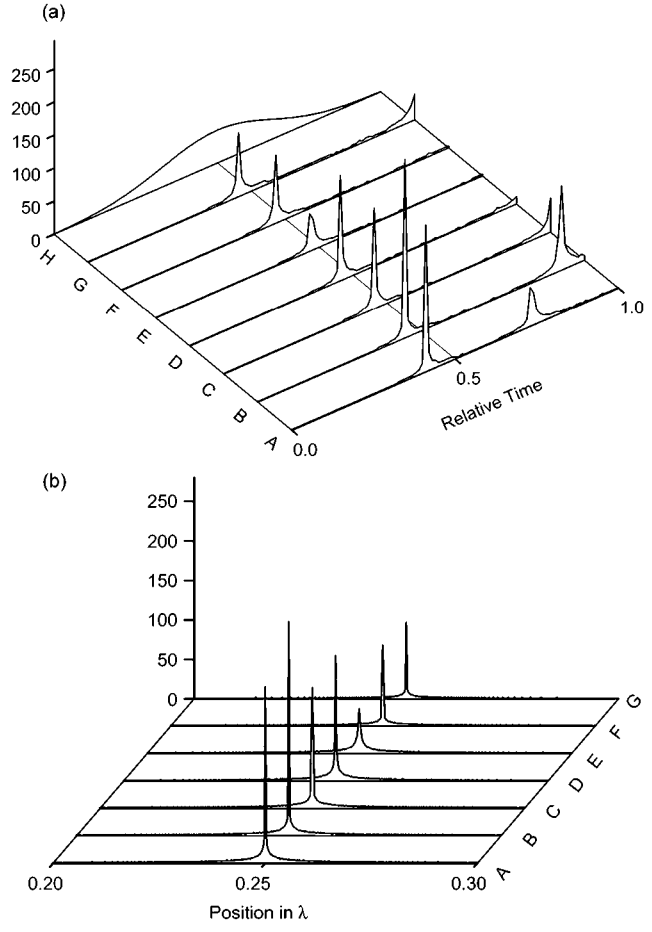

Figure 6. Same as with Fig. 4 but calculated with the CPO approach. The focal planes deviate from the Gaussian center of the potential, and slower beams tend to be better as opposed to quantum mechanical predictions.

unoptimized (or CPO optimized).

Figure 6 shows the results of CPO simulations with the same parameters as the quantum mechanical ones. We find that the laser powers optimized for quantum mechanical simulations are not optimal for CPO: the focal planes deviate from the Gaussian center of the potential and slower beams tend to perform better as opposed to quantum mechanical results. Therefore, CPO-based analysis of the atom lithography may lead to erroneous predictions.

Conclusions

In this paper we analyzed focusing of an atomic beam in a laser standing wave. By integrating both a classical ray-tracing equation and a coupled Schrödinger equation, we compared classical and quantum mechanical behavior of a Cr atomic beam in a focusing laser. We found that current experimental parameters are optimal in the context of particle optics, but they are not optimal when the wave nature of atom is considered. Since the atom focusing depends on both the force field to which atoms are subject and the length of time atoms experience the field, we took the variation of the atomic beam speed into consideration and optimized the laser power accordingly. It is shown that the analysis based on the classical particle optics approach, which doe not incorporate the wave nature of atom, is at variance with what quantum mechanics predicts and, therefore, is not dependable. It is found that by doubling the atomic beam speed along with an optimized laser power, much smaller spot size about 3.8 nm can be obtained, if all the classical source of imperfections are removed. Faster beam speed coupled with higher contrast means higher throughput-that is, higher deposition rate, which may be important in mass production. These parameters are readily available with the current technology.

Acknowledgments. This work was supported by the '2001 institutional research fund of Sunmoon University.

References

1. Timp, G. *et al. Phys. Rev. Lett.* **1992**, *69*, 1636.
2. McClelland, J. J. *et al. Science* **1993**, *162*, 877.
3. Prentiss, M.; Timp, G.; Bigelow, N.; Behringer, R. E.; Cunningham, J. E. *Appl. Phys. Lett.* **1992**, *60*, 1027.
4. Seideman, T. In *Molecular Optics in Intense Fields: From Lenses to Mirrors, in Molecular Beams*; Campargue, R. Ed.; Springer-Verlag: Berlin, 2001; p 133; *Phys. Rev. A* **1997**, *56*, R17; *J. Chem. Phys.* **1997**, *106*, 2881; **1997**, *107*, 10420; **1999**, *111*, 4113.
5. Nowad, S.; Pfau, T.; Mlynek, J. *Appl. Phys. B: Lasers Opt.* **1996**, *63*, 203.
6. Nowad, S.; Pfau, T.; Mlynek, J. *Phys. Rep.* **1994**, *240*, 143.
7. McClelland, J. J. *et al. Aust. J. Phys.* **1996**, *49*, 555, and references therein.
8. McClelland, J. J. *J. Opt. Soc. B* **1995**, *12*, 1761.
9. Anderson, W. R. *et al. Phys. Rev. A* **1999**, *59*, 2476.
10. Lee, C. J. *Phys. Rev. A* **2000**, *53*, 4056.
11. Dalibard, J.; Cohen-Tannoudji, C. *J. Opt. Soc. Am. B* **1985**, *2*, 1707.
12. See, for example, Chu, S.; Wieman, C. E. *J. Opt. Soc. Am. B* **1989**, *6*, 2020.
13. Cohen-Tannoudji, C. In *Fundamental Systems in Quantum Optics*; Dalibard, J., Raimond, J.-M., Zinn-Justin J., Eds.; North-Holland: Amsterdam, 1992; p 1.
14. Ashkin, A. *Phys. Rev. Lett.* **1978**, *40*, 729.
15. Kidan, T.; Adler, J.; Ron, A. *Computers in Physics* **1998**, *12*, 471.
16. In this paper we consider the transverse range $-1.28\lambda \le x \le 1.28$ lambda . Thus, all atomic densities at any time are normalized so that int from $\int_{-1.28\lambda}^{1.28\lambda} |\Psi(x)|^2 dx = 1$.